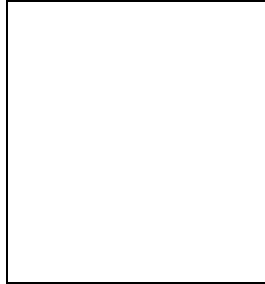


Hydrodynamical Simulations of the Sunyaev Zel'dovich effect

Antonio C. da Silva,¹ Domingos Barbosa,² Andrew R. Liddle¹ and Peter A. Thomas¹

¹*Astronomy Centre, University of Sussex, Brighton BN1 9QJ, United Kingdom*

²*Lawrence Berkeley Laboratory, 1 Cyclotron Road, Berkeley CA 94710, USA*



The Sunyaev–Zel'dovich (SZ) effect is reaching observational maturity. Future experiments, with higher sensitivities and larger frequency coverage, will measure this effect for a large number of clusters and may detect the overall level of SZ distortions to the CMB background. Given that, it is crucial to establish detailed theoretical predictions to interpret observations. We have used hydrodynamical N-body simulations to construct maps of the SZ effect for three popular CDM cosmologies. The study of these maps enabled us to make predictions for a range of properties, such as the mean thermal distortion and source counts at a series of different angular resolutions, including that of the PLANCK satellite.

1 Introduction

The Sunyaev–Zel'dovich (SZ) effect (Sunyaev & Zel'dovich 1972, 1980; for reviews see Rephaeli 1995 and Birkinshaw 1999) arises due to the inverse Compton scattering of the Cosmic Microwave Background (CMB) photons by a hot ionized gas of electrons, especially that in galaxy clusters. As the radiation propagates through these ionized regions, a fraction of the original CMB photons scatter off the moving electrons and suffer doppler frequency shifts. The SZ effect can be divided in two components: the thermal SZ effect, due to the thermal motion of the electrons, and the kinetic SZ effect due to the bulk velocity of the gas. The dominant contribution is the thermal effect. As the gas is very hot (commonly at $T \simeq 10^8\text{K}$ in clusters) the scattered photons gain energy and move towards higher frequencies. This produces an excess of photons in the Wien spectral region and a decrement of intensity in the Rayleigh–Jeans side of the CMB spectrum. The thermal SZ is described by the y -Compton parameter and its amplitude is proportional to an integral along the line of sight of the product of the electron density and the temperature ($y \propto \int T_e n_e dl$). Therefore, spectral distortions are stronger and easier to detect in the direction of hot dense clusters of galaxies.

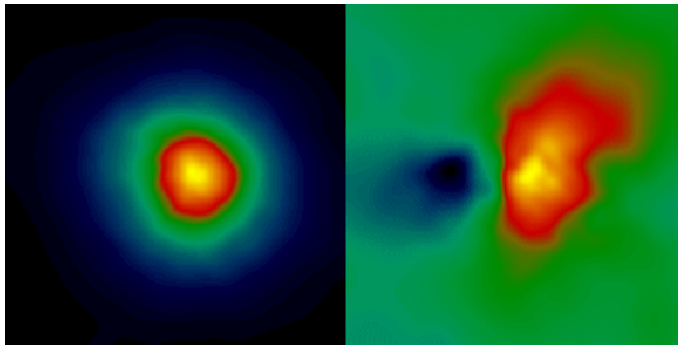


Figure 1: Simulated temperature fluctuation maps of the thermal (on the left) and kinetic (on the right) SZ effect in the direction of a cluster. The color scales were chosen to enhance the effects. Their ranges are $[0, 1] \times 10^{-4}$ in the thermal map and $[-5, 5] \times 10^{-6}$ in the kinetic map.

SZ detections towards known clusters are now becoming routine. Several instruments are capable of making two-dimensional maps and blank-field surveys are being proposed to probe extended regions in the sky. An all-sky catalog, containing thousands of SZ sources, will be made by the upcoming satellite mission PLANCK. It is vital to establish accurate theoretical predictions to interpret the observational results. Up until now, the preferred theoretical tool has been the Press–Schechter (PS, 1974) approach. Although in good agreement with previous numerical simulations, this involves a number of approximations (e.g. spherical symmetry and virialization of the PS halos, often taken to have isothermal temperature profiles). To avoid these drawbacks, we have studied the SZ effect using hydrodynamical N -body simulations. Figure 1 shows simulated thermal and kinetic SZ maps, of size 20 arcminutes, taken in the direction of a cluster in an $\Omega_0 = 1$ simulation. The temperature distortions were integrated along the line of sight for a single simulation box at redshift $z = 0.31$ and thickness $dz = 0.08$. Whereas the thermal map shows a reasonable spherical symmetry, the kinetic map (which is only dependent on the velocity and density of the gas particles) is asymmetric, with regions of both blueshift and redshift. This may suggest the overlap of a bright source with a distant faint one or, more likely, a merging event of substructures in a major and clearly not relaxed cluster.

As well as applications in the study of individual clusters, the SZ effect has also long been regarded as a promising cosmological probe, through the use of “sky” statistics such as SZ source counts. Of particular importance to future CMB experiments is to determine whether the SZ effect is a significant source of foreground contamination to the CMB. We have created simulated SZ maps to estimate the mean distortion level and other SZ properties like source counts at different angular resolutions, for three CDM cosmologies.

2 Simulations and map making technique

We used the public domain code `Hydra` (Couchman et al. 1995), an Adaptive P³M algorithm to compute the gravitational forces with Smoothed Particle Hydrodynamics to follow the gas dynamics, to generate a set of three simulations, one for each of the following cosmologies: a Λ CDM model with $\Omega_0 = 0.35$, $\Omega_\Lambda = 0.65$; a τ CDM model with $\Omega_0 = 1$, $\Omega_\Lambda = 0$; and an open model OCDM with $\Omega_0 = 0.35$, $\Omega_\Lambda = 0$. In each case, the box-size was $150 h^{-1}$ Mpc, equal numbers of dark matter and gas particles were used and the normalization σ_8 of the CDM power spectrum was chosen to ensure good agreement with the observed cluster abundances. The simulation output is a set of boxes at different redshifts, which stack smoothly in an evolving sequence. To construct maps, of size 1 square degree, we proceed as follows: for a given box, using the periodical boundary conditions of the simulations, the particle positions are trans-

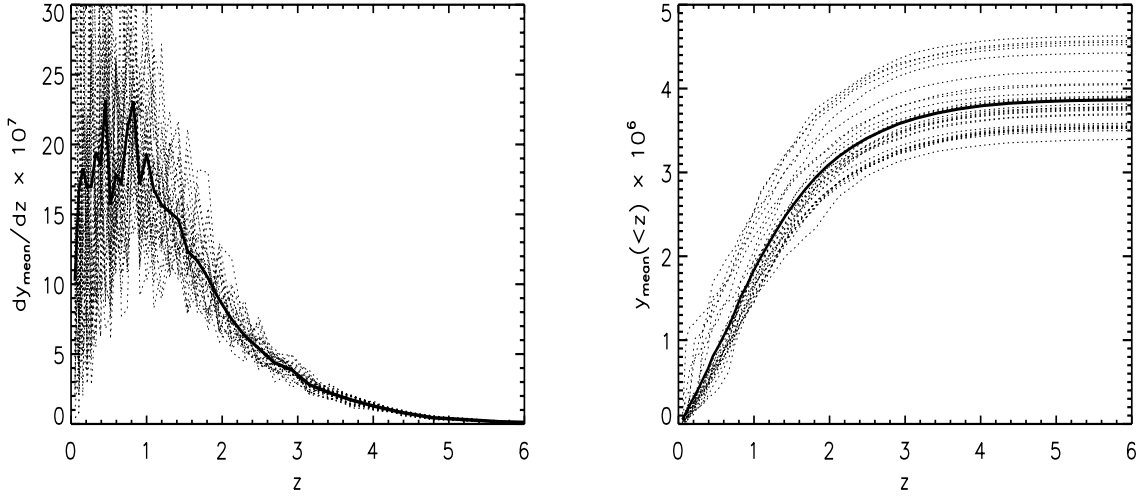


Figure 2: Contribution of different redshifts to the mean y distortion in the Λ CDM simulation. Left panel: differential contribution per unit redshift. Right panel: integrated contribution out to redshift z . In each case the solid line is the average over the 30 maps represented by the dotted lines.

lated by a random amount and rotated by multiples of 90° about each axis (this has to be done due to the fact we have only one simulation per cosmology). Then we compute the angular diameter distance to the box, to obtain the size of the map at that redshift and integrate the SZ distortions along the box length. The operation is repeated for consecutive boxes and the partial maps are accumulated. In order to ensure that all significant contributions are included, one has to go to high enough redshift. Typically around 40 boxes are stacked. However in the nearby boxes only a small fraction of the volume of the box contributes to the maps and so we do not expect significant problems from having only a single hydrodynamical simulation. In practice, we make 30 different maps for each cosmology, corresponding to different random symmetry operations over the stacked simulations. Further details about the simulations, map making strategy and expressions used to evaluate numerically the SZ distortions can be found in da Silva et al. (2000).

3 Results

The mean SZ distortion arises due to the cumulative effect of hot gas across the sky. The present observational limit was set by the COBE–FIRAS experiment, $y_{\text{mean}} < 1.5 \times 10^{-5}$ (95% CL), Fixen et al. (1996). All our simulations are below this limit. We found $y_{\text{mean}} = 1.3 \times 10^{-6}$, 3.9×10^{-6} and 3.3×10^{-6} for the τ CDM, Λ CDM and OCDM cosmologies, respectively. Figure 2 shows the contribution of different redshifts to y_{mean} , for 30 map realizations, in the Λ CDM cosmology. The total mean y up to a given z in the right panel is the area under the curves to the same redshift on the left panel. Notice the significant dispersion between realizations. This happens due to the chance of having bright sources in the volumes enclosed by the map at low z . The mean distortion from nearby boxes comes mainly from rare bright sources, whereas at large distances it is due to larger numbers of fainter ones. Simulations show that in low-density cosmologies, the y_{mean} is contributed across a wide range of redshifts, with the bulk coming from $z < 2$ and a tail out to $z \sim 5$. In the τ CDM case most of the contribution comes from $z < 1$.

The left panel in figure 3 shows a histogram of the averaged pixel distribution in the thermal maps for the Λ CDM cosmology. The different curves represent different gaussian smoothings

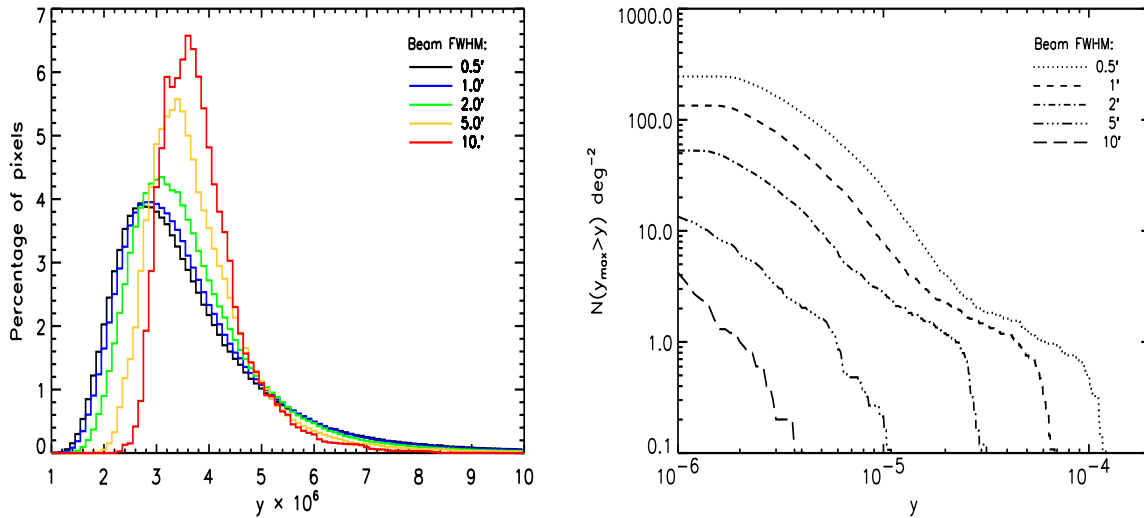


Figure 3: Pixel distribution of the y parameter in the thermal maps (left panel) and source counts above a given central y_{max} (left panel) for different gaussian beam smoothings in the Λ CDM simulation.

ranging from (top to bottom) 10' to 0.5' (FWHM). The curves show the expected y values which would be seen if an instrument with the corresponding resolution points randomly at the sky. As expected, increased smoothing narrows down the width of the distributions around y_{mean} . The right panel of figure 3 shows the average number of sources per square degree with a maximum exceeding a given y_{max} in the Λ CDM simulation. The different curves represent different beam smoothings, corresponding loosely to different experimental resolutions. The counts were produced with a source extraction code based on a connected-pixel algorithm (Bertin & Arnouts, 1996). For low y the curves flatten out because the routine becomes source confused. The bumps shown for high values of y are due to cosmic variance: although we average over many map realizations we have only one simulation per cosmology. The number of SZ sources above a given y depends strongly on instrument resolution and on cosmology. As an example, for a 1' beam, the simulations show ~ 0.1 sources/deg² with $y > 10^{-5}$ in a τ CDM universe, and ~ 8 such sources/deg² in low-density models. The Λ CDM and OCDM models give very similar results. Based on the simulated number counts we estimate that PLANCK will be able to detect around 25000 SZ sources if the Universe has a low density, or around 10000 if it has critical density.

Acknowledgments

ACdS was supported by FCT (PRAXIS XXI BD/11059/97 Portugal), DB by the European Union TMR programme, ARL in part by the Royal Society, and PAT by a PPARC Lecturer Fellowship. We acknowledge use of the Starlink computer system. Simulations were carried out on the BFG-HPC facility at Sussex funded by HEFCE and SGI, and part of the data analysis on the COSMOS National Cosmology Supercomputer funded by PPARC, HEFCE and SGI.

References

1. Sunyaev R. A., Zel'dovich Ya. B., 1972, *Comm. Astrophys. Space Phys.*, 4, 173
2. Sunyaev R. A., Zel'dovich Ya. B., 1980, *ARA&A*, 18, 537
3. Rephaeli Y., 1995, *ARA&A*, 33, 541
4. Birkinshaw M., 1999, *Phys. Rep.*, 310, 98

5. Press W. H., Schechter P., 1974, ApJ, 187, 425
6. Couchman H. M. P., Thomas P. A., Pearce F. R., 1995, ApJ, 452, 797
7. da Silva A., Barbosa D., Liddle A., Thomas P., 2000, astro-ph/9907224, to appear, MNRAS
8. Fixsen D. J. et al., 1996, ApJ, 473, 576
9. Bertin E., Arnouts S., 1996, A&AS, 117, 393